

The performance investigation of viscoelastic hybrid models in vehicle crash event representation

Witold Pawlus,* Kjell Gunnar Robbersmyr,*
Hamid Reza Karimi,* Arnfinn Fanghol*

* *The University of Agder, Faculty of Engineering and Science, Postbox 509, N-4898 Grimstad, Norway (e-mail: witolp09@student.uia.no, {kjell.g.robbersmyr; hamid.r.karimi; arnfinn.fanghol}@uia.no).*

Abstract: This paper presents application of physical models composed of springs, dampers and masses joined together in various arrangements to simulation of a real car collision with a rigid pole. Equations of motion of those systems are being established and subsequently solutions to obtained differential equations are formulated. We start with a general model consisting of two masses, two springs, and two dampers, and illustrate its application to represent fore-frame and aft-frame of a vehicle. Hybrid models, as being particular cases of two mass-spring-damper model, are elaborated afterwards and their application to predict results of real collision is shown. Models' parameters are obtained by fitting their response equations to the real vehicle's crush coming from the acceleration measurement analysis. For full-scale experiment and created models we perform both: kinematic and energy responses comparative analysis.

Keywords: Vehicle crash, energy absorbers, hybrid models, kinematics, modeling.

1. INTRODUCTION

Vehicle crash modeling is one of the paramount challenges in the area of crashworthiness. Every car which is going to appear on the roads must undergo a series of complex and expensive crash tests to verify whether it conforms to the relevant safety standards and regulations. Hence it is of great interest to propose a mathematical model which can represent a full-scale collision and provide results which will be used instead of the experiment outcome.

Recently we can distinguish two main approaches of vehicle crash modeling: FEM (Finite Element Method) simulations and mathematical LPM (Lumped Parameter Modeling). References Borovinsek et al. (2007), Harb et al. (2007), and Soica and Lache (2007) provide brief overview of different crash modes. In Varat and Husher (2000) there are presented basic mathematical functions (like sine, haversine or square wave pulse) used to simplify the crash acceleration. Another manner of expressing the measured acceleration signal as an approximation is wavelet application. Haar wavelets have been employed in Karimi and Robbersmyr (2011) to create the equivalent plot of the crash pulse.

Even in the domain of FEM which could be considered as the most robust and authoritative tool in vehicle crash simulation there are continuously being done upgrades. In Eskandarian et al. (1997) a Bogie instead of a real car was modeled in a software and its behavior was compared to the real experiment's results. In the work done by Tenga et al. (2008) the multibody occupant model was constructed and its response for the crash pulse was compared with the full-scale FE model (LS-DYNA3D).

References Kim et al. (1996), Soto (2004), and Moumni and Axisa (2004) illustrate how the complicated, complete mesh model of a car can be further decomposed into less complex arrangements.

On the other hand, LPM is an analytical method of formulating a model which can be further used for simulation of a real event. It allows us to establish dynamic equations of the system - differential equations - which give the complete description of the models behavior, see Deb and Srinivas (2008) and Jonsén et al. (2009). In Pawlus et al. (2010b) and Pawlus et al. (2010c) basic mathematical models of vehicle to pole collision are created. Full-scale experiment described by Robbersmyr (2004) has been analyzed and modeled - simulation results proved the effectiveness of established models in representing vehicle localized impact. In the most up-to-date scope of research concerning crashworthiness it is to define a dynamic vehicle crash model which parameters will be changing according to the changeable input (e.g. initial impact velocity). One of such trials is presented in van der Laan et al. (2008) - a non-linear occupant model is established and scheduling variable is defined to formulate LPV (linear parametrically varying) model.

Vehicle crash investigation is an area of up-to-date technologies application. References Givotto et al. (1983), Harmati et al. (2008), and Omar et al. (1998) discuss usefulness of such developments as neural networks or fuzzy logic in the field of modeling of crash events. Those two intelligent technologies have extremely high potential for creation of vehicle collision dynamic models and their parameters establishment - e.g. in Pawlus et al. (2010a) values of spring stiffnesses and damping coefficients for

lumped parameter models (LPM) were determined by the use of radial basis artificial neural network (RBFN) and the responses generated by such models were compared with the ones obtained via analytical solutions. Fuzzy logic together with neural networks and image processing have been employed by Várkonyi-Kóczy et al. (2004) to estimate the total deformation energy released during a collision. A vision system has been developed to record a crash event and determine relevant edges and corners of a car undergoing deformation. In addition to this work, in Elmarakbi and Zu (2006) one can find a complete derivation of vehicle collision mathematical models composed of masses and piecewise nonlinear springs and dampers.

One of the main contributions of this paper is the evaluation of the presented vehicle crash modeling principles with the full-scale experimental data analysis. Models shown in this work have higher degree of complexity due to the fact that they are composed of totally 3 energy absorbers (EA). This approach is a next step towards the multi-body systems utilized for simulation of particular car components behavior or interactions between a car and an occupant.

This paper presents a way to create a model of a vehicle crash based on viscoelastic properties of materials. System proposed by us is composed of a mass, two springs and one damper in two different configurations (so called hybrid model). Derivation of equations of motion (EOM) for two mass-spring-damper model and hybrid model are shown. Subsequently, models application to simulate the real experiment is evaluated.

2. TWO MASS-SPRING-DAMPER MODEL

This model, presented in Fig. 1, simulates a rigid barrier impact of a vehicle where m_1 and m_2 represent the frame rail (chassis) and passenger compartment masses, respectively. Another application of such an arrangement may be description of relationships between vehicle structure (m_1) with energy absorbers (spring with stiffness k_1 and damper with coefficient c_1) and occupant torso (m_2) with restraint system of spring k_2 and damper c_2 - see Huang (2002). Particular displacements of masses m_1 and m_2 are denoted as x_1 and x_2 , respectively.

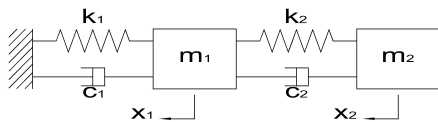


Fig. 1. A two mass-spring-damper model

2.1 Equations of motion

The equations of motion (EOM) of this system are shown in (1) and (2).

$$m_1 \ddot{x}_1 + (c_1 + c_2) \dot{x}_1 + (k_1 + k_2)x_1 - c_2 \dot{x}_2 - k_2 x_2 = 0 \quad (1)$$

$$m_2 \ddot{x}_2 + c_2 \dot{x}_2 + k_2 x_2 - c_2 \dot{x}_1 - k_2 x_1 = 0 \quad (2)$$

2.2 Characteristic equation and its solutions

The following characteristic equation of the two mass-spring-damper model (4th order polynomial) has been obtained:

$$s^4 + ts^3 + us^2 + vs + w = 0 \quad (3)$$

where:

$$t = \frac{m_1 c_2 + m_2 (c_1 + c_2)}{m_1 m_2}, \quad u = \frac{m_1 k_2 + m_2 (k_1 + k_2 + c_1 c_2)}{m_1 m_2},$$

$$v = \frac{k_1 c_2 + k_2 c_1}{m_1 m_2}, \quad \text{and} \quad w = \frac{k_1 k_2}{m_1 m_2}.$$

2.3 Model simulation

Since the derivation of displacement and velocity formulas for the two mass-spring-damper model is complex procedure and is in details covered in Huang (2002) we do not present it here. We directly proceed to an exemplary configuration which can be used to simulate vehicle to rigid barrier collision. Parameters of this model have been selected for a typical mid-size vehicle according to Huang (2002) - they do not come from an experiment. Whole vehicle was divided into two parts: m_1 - which represents mass of the vehicle's fore-frame and m_2 - which represents mass of the vehicle's aft-frame. Let us assume the following numerical values: $m_1 = 450kg$, $m_2 = 900kg$, $c_1 = 13300N \cdot s/m$, $c_2 = 9800N \cdot s/m$, $k_1 = 1099000N/m$, $k_2 = 693000N/m$ and initial impact velocity $v_0 = 50km/h$. Characteristic equation looks like this:

$$s^4 + 62s^3 + 5074s^2 + 49350s + 1880511 = 0.$$

By following the same methods as the ones shown in Huang (2002) we obtain the set of coefficients (roots, amplitudes and phase angles) describing the motion of the particular masses - response of the model is plotted in Fig. 2.

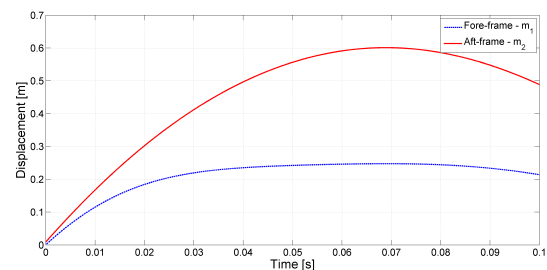


Fig. 2. Exemplary responses of a two mass-spring-damper model

Those two responses are plotted in the absolute reference frame. Such characteristic is justified from the engineering point of view: the front part of the vehicle undergoes smaller deformation than the rear one. What is more, the time at which the maximum fore-frame displacement occur is much shorter than for the aft-frame because of its additional compression by the rest of the car. We may also observe that the rebound occurs starting from the rear portion of the vehicle: fore-frame starts to move back from the barrier only when the aft-frame is already moved by a significant distance.

3. HYBRID MODELS

Hybrid models from Fig. 3 and Fig. 4 are simplified two mass-spring-damper models - one damper has been detached and m_1 has been set to zero. The following notation have been used: c - damping coefficient, k_1 and k_2 - spring stiffnesses, m_e - equivalent mass, it will be further denoted simply as m , v_0 - initial impact velocity, x_0 and x_1 - absolute displacements of a junction point and mass, respectively. A hybrid model is a combination of Maxwell and Kelvin models. Its elements (two springs and one damper) are connected in such a way that the two hybrid models are structurally and functionally different (non-isomorphic).

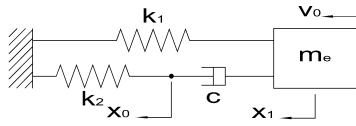


Fig. 3. 1st hybrid model

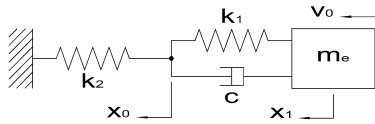


Fig. 4. 2nd hybrid model

3.1 Equations of motion

Derivation of EOM for hybrid models is similar to the one presented for two mass-spring-damper model. We start from formulating dynamic equations with the small mass m_1 placed in the junction point. We establish EOM separately for each mass in each of the two hybrid models. Subsequently we set m_1 to zero, differentiate every equation and substitute its displacement variable x_0 together with its derivative (velocity) to get EOM expressed as a function of just one variable x_1 - displacement of the mass m and its derivatives: \dot{x}_1 , \ddot{x}_1 , and $\ddot{\dot{x}}_1$, respectively.

EOM for 1st hybrid model

$$\ddot{\dot{x}}_1 + \frac{k_2}{c} \ddot{x}_1 + \frac{k_1 + k_2}{m} \dot{x}_1 + \frac{k_1 k_2}{cm} x_1 = 0 \quad (4)$$

EOM for 2nd hybrid model

$$\ddot{\dot{x}}_1 + \frac{k_1 + k_2}{c} \ddot{x}_1 + \frac{k_2}{m} \dot{x}_1 + \frac{k_1 k_2}{cm} x_1 = 0 \quad (5)$$

3.2 Characteristic equation

By taking Laplace transform of (4) and (5) with initial conditions equal to zero and substituting the model parameters (m , c , k_1 , and k_2) by the coefficients t , u , and v we obtain the following characteristic equation of above two hybrid models:

$$s^3 - ts^2 + us - v = 0. \quad (6)$$

Equivalents of coefficients t , u , and v in terms of models parameters are shown in Table 1.

Table 1. Characteristic equation's coefficients equivalence between hybrid models

Model	t [1/s]	u [1/s ²]	v [1/s ³]
1st	$-\frac{k_2}{c}$	$\frac{k_1 + k_2}{m}$	$-\frac{k_1 k_2}{cm}$
2nd	$-\frac{k_1 + k_2}{c}$	$\frac{k_2}{m}$	$-\frac{k_1 k_2}{cm}$

3.3 Dynamic equivalence between two non-isomorphic hybrid models

By appending a subscript i to the existing models' coefficients ($i = 1, 2$ and designates the corresponding hybrid model) two sets of energy absorbers (springs and dampers) become unique for each model (Huang (2002)). Since there are three constraint equations for t , u , and v , and three unknowns (let us assume k_{11} , k_{21} , and c_1) we may write the following equivalence formulas:

$$k_{11} = \frac{k_{12} k_{22}}{k_{12} + k_{22}} \quad (7)$$

$$k_{21} = \frac{k_{22}^2}{k_{12} + k_{22}} \quad (8)$$

$$c_1 = \frac{k_{22}^2}{(k_{12} + k_{22})^2} c_2. \quad (9)$$

Dynamic equivalence between those two models applies only to the kinematic, crush, and energy responses of the masses. There is no equivalence among the corresponding energy absorbers (Huang (2002)). Thanks to (7) to (9), it is possible to quickly switch between the hybrid models. Having parameters of one of them, we are able to easily get the parameters of the another one.

3.4 Responses of hybrid models

Since the characteristic equation (6) is a third order polynomial which coefficients can have just certain values (because they describe a real physical system) it was found that the only possible configuration of its solutions is one real root β and two complex conjugate roots $\epsilon + i\omega$ and $\epsilon - i\omega$ (stable system). Let us introduce the following relationships:

$$\epsilon = \frac{u - \frac{v}{\beta}}{2\beta}$$

$$\omega = \sqrt{\left| \epsilon^2 - \frac{v}{\beta} \right|}$$

$$p = v_0 \cdot \frac{2\epsilon}{(\beta - \epsilon)^2 + \omega^2}$$

$$q = v_0 \cdot \frac{\beta^2 - \epsilon^2 + \omega^2}{\omega [(\beta - \epsilon)^2 + \omega^2]}$$

where β , ϵ , and ω are in [rad/s]. Taking advantage of above formulas we define the displacement, velocity and acceleration of hybrid models, respectively (when we take

into account initial conditions at $t = 0$: $x_1 = 0$, $\dot{x}_1 = v_0$, and $\ddot{x}_1 = 0$ we will de facto obtain a particular solution for third order differential equation - EOM of hybrid model - and its two derivatives):

$$\alpha = -pe^{\beta t} + e^{\epsilon t}(p \cos \omega t + q \sin \omega t) \quad (10)$$

$$\dot{\alpha} = -p\beta e^{\beta t} + e^{\epsilon t}[\epsilon(p \cos \omega t + q \sin \omega t) - \omega(p \sin \omega t - q \cos \omega t)] \quad (11)$$

$$\ddot{\alpha} = -p\beta^2 e^{\beta t} + e^{\epsilon t}[(\epsilon^2 - \omega^2)(p \cos \omega t + q \sin \omega t) - 2\epsilon\omega(p \sin \omega t - q \cos \omega t)]. \quad (12)$$

4. EXPERIMENT DESCRIPTION

The experiment which results we were using in the research was a typical mid-speed vehicle to pole collision. Its elaboration presented here has been done according to Robbersmyr (2004). A test vehicle was subjected to impact with a vertical, rigid cylinder. The acceleration field was 100 meter long and had two anchored parallel pipelines. The vehicle was steered using those pipelines that were bolted to the concrete runaway. Setup scheme is shown in Fig. 5.

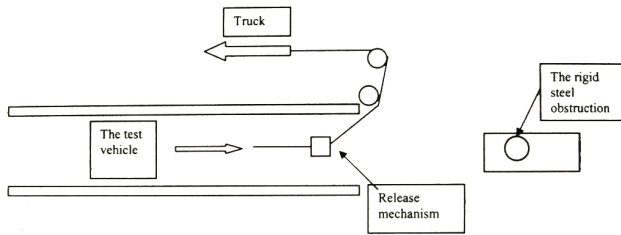


Fig. 5. Experimental setup (Robbersmyr (2004))

During the test, the acceleration was measured in three directions (x - longitudinal, y - lateral, and z - vertical) together with the yaw rate from the center of gravity of the car. Using normal speed and high - speed video cameras, the behavior of the safety barrier and the test vehicle during the collision was recorded. The initial velocity of the car was 35 km/h, and the mass of the vehicle (together with the measuring equipment and dummy) was 873 kg. The obstruction was constructed with two steel components - a pipe filled with concrete and a baseplate mounted with bolts on a foundation. The car undergoing the deformation is shown in Fig. 6.



Fig. 6. Car during a collision (Robbersmyr (2004))

5. MODEL ESTABLISHMENT

Having in our disposal acceleration measurement from the experiment we integrate it twice (since it is a frontal collision we analyze only x-direction - longitudinal) and obtain the vehicle's displacement history.

5.1 Curve fitting

We fit previously established response of a hybrid model (10) to the real car's crush. However, coefficients in (10) resulting from the fitting procedure do not necessarily follow the relationships among model's parameters presented in Table 1 and Section 3.4. Therefore we need to express (10) only in terms of t , u , and v because only then we will be able to calculate the unique values of parameters k_1 , k_2 , and c , according to Table 1. This is possible since variables p , q , ϵ , ω , and root β are functions of the characteristic equation's coefficients t , u , and v . Equation obtained from such reasoning becomes very long. Software used for performing the fit was Matlab Curve Fitting Toolbox.

Boundaries for coefficients t , u , and v In order to efficiently determine parameters of our modified equation (t , u , and v) we need to provide reasonable ranges of their values. From considerations shown in Table 1 we conclude that $t < 0$, $v < 0$, and $u > 0$ (since all the models' parameters k_1 , k_2 , m , and c are positive). If we further analyze formulas from Table 1 we are able to establish relationships among particular equation's coefficients by using above basic dependencies. Finally we came up with the following two additional constraints valid for both hybrid models:

- (1) $ut < v < 0$
- (2) $vm < t < 0$.

Determination of coefficients t , u , and v Fitting results are presented in Fig. 7. The root mean squared error (RMSE) for this fit is equal to $RMSE = 0.02278$, whereas the sum of squared errors is equal to $SSE = 0.9079$. Model's equation parameters obtained via this method are listed in Table 2. As we see they satisfy the constraints established in Section 5.1.1. Please note that the mass in the hybrid model remains the same as the mass of the real vehicle, i.e. $m = 873kg$.

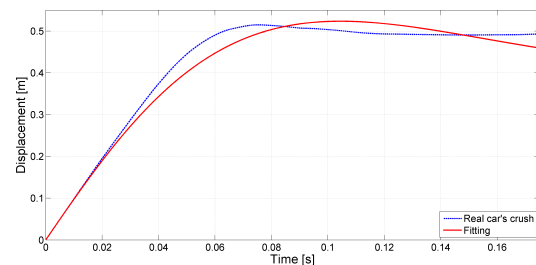


Fig. 7. Outcome of the fitting procedure

5.2 Models creation

By taking advantage of formulas from Table 1 we calculate the following values of hybrid models' particular coefficients - see Table 3.

Table 2. Coefficients of the characteristic equation obtained by curve fitting

t [1/s]	u [1/s ²]	v [1/s ³]
-32.75	684.60	-500.00

Table 3. Hybrid models' parameters

Model	k_1 [N/m]	k_2 [N/m]	c [N · s/m]	m [kg]
1st	13328	584330	17842	873
2nd	13632	597660	18665	873

We see that all in all the corresponding parameters of two different hybrid models do not differ much from each other. According to the reasoning elaborated in Section 3.3 we state that those two non-isomorphic systems exhibit the same kinematic, crush, and energy behavior.

5.3 Models simulation

Kinematic responses Results are presented in Fig. 8 to Fig. 10.

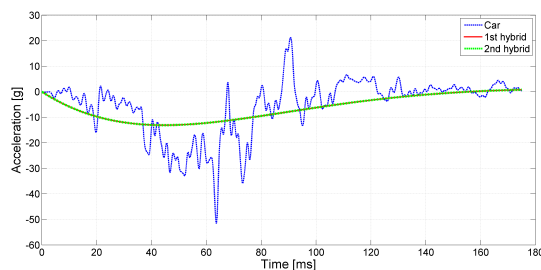


Fig. 8. Comparative analysis between hybrid models' and real car's acceleration

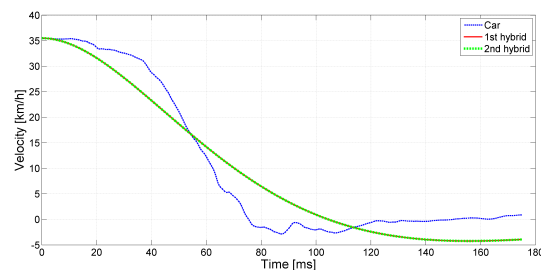


Fig. 9. Comparative analysis between hybrid models' and real car's velocity

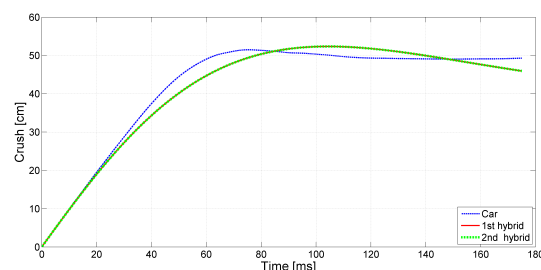


Fig. 10. Comparative analysis between hybrid models' and real car's crush

Plots confirm that indeed two different hybrid models which corresponding parameters are related to each other by the formulas from Table 1 generate the same kinematic

responses. The overall behavior of the models match the real car's crush, velocity, and acceleration time histories well. Two of the main parameters characterizing the collision are: the maximum dynamic crush C - which describes the highest car's deformation, and the time at which it occurs - t_m . They are pertinent to the occupant crashworthiness since they help to assess the maximum intrusion to the passenger's compartment and they influence the airbag activation time. In Table 4 one can find values of C and t_m for both: model and real collision.

Table 4. Maximum dynamic crush and time comparison

	C [cm]	t_m [ms]
Real car	51	76
Hybrid models	52	104

Deformation predicted by the model is almost the same as the one coming from the experiment, whereas the time at which it occurs is 36% higher than the real one. However, the overall characteristics produced by the model stay in accordance with the reference ones.

Energy responses According to Huang (2002) let us introduce the following formula for coefficient of restitution (considerations presented below are valid for central impact with one dimensional motion):

$$e = \frac{\text{relative separation velocity}}{\text{relative approach velocity}} = \frac{v'}{v}. \quad (13)$$

Perfectly elastic collision results with $e = 1$ (no energy loss), whereas for totally dissipative collision $e = 0$. In that case the separation velocity is zero - this corresponds to the collision of two vehicles which after the impact move as one body or to the impact with a rigid obstruction (e.g. a barrier). Energy relationships are given by:

$$\Delta E' = (1 - e^2) \left[\frac{1}{2} m v^2 \right] \quad (14)$$

$$\Delta E = \left[\frac{1}{2} m v^2 \right] \quad (15)$$

$$\Delta E' = (1 - e^2) \Delta E. \quad (16)$$

In general ΔE is the total crush energy absorbed by the two colliding vehicles and $\Delta E'$ is the total crush energy dissipated by them. In the rigid barrier impact, the total energy absorbed by the structure is the same as the total crush energy shown in (15). Fig. 11 presents crush energy changes during a collision for both: real car and hybrid models' mass. As one could expect, since crush energy E is a function of velocity v , the overall shapes of the plots resemble those of velocity from Fig. 9.

6. CONCLUSION

Two hybrid models with good fidelity have been established in this paper to simulate a certain vehicle crash event. The conditions for their equivalence have been presented, thus one can use them interchangeably. Even if they are non-isomorphic, they are capable to represent

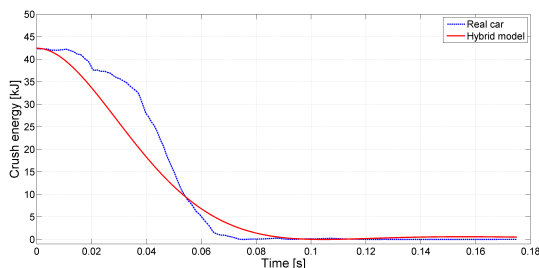


Fig. 11. Crush energy comparison

the each other's behavior. By analyzing the collision from the energetic point of view, it is concluded that a stiffer vehicle absorbs less of the total crush energy. On one hand it results in decreasing the intrusion to the passenger's compartment, but on the other hand it produces higher occupant's acceleration (so automatically increases occupant crash severity). Therefore car design is a trade-off between structural and geometrical parameters of a vehicle and desired safety of driver and passengers. Future work in this area may cover development of a method which lets establish relationships between mathematical models parameters and vehicle initial impact velocity. This is particularly desirable since all the models shown here are LPM (Lumped Parameter Models) valid just for the one given impact speed. For that reason they cannot be used to effectively predict car's behavior in a variety of impact scenarios. Neural networks or fuzzy logic may be appropriate tools in this challenge, since they deal well with the non-linear systems modeling.

REFERENCES

- Borovinsek, M., Vesenjok, M., Ulbin, M., and Ren, Z. (2007). Simulation of crash tests for high containment levels of road safety barriers. *Engineering Failure Analysis*, 14(8), 1711–1718.
- Deb, A. and Srinivas, K.C. (2008). Development of a new lumped - parameter model for vehicle side - impact safety simulation. In *Proceedings of the Institution of Mechanical Engineers, Part D: Journal of Automobile Engineering*, volume 222, 1793–1811. Professional Engineering Publishing. ASME.
- Elmarakbi, A.M. and Zu, J.W. (2006). Crash analysis and modeling of two vehicles in frontal collisions using two types of smart front-end structures: an analytical approach using IHB. *International Journal of Crashworthiness*, 11, 467–483.
- Eskandarian, A., Marzougui, D., and Bedewi, N.E. (1997). Finite element model and validation of a surrogate crash test vehicle for impacts with roadside objects. Technical report, National Crash Analysis Center, Virginia, USA.
- Giavotto, V., Puccinelli, L., Borri, M., Edelman, A., and Heijer, T. (1983). Vehicle dynamics and crash dynamics with minicomputer. *Computers and Structures*, 16(1-4), 381–393.
- Harb, R., Radwan, E., Yan, X., and Abdel-Aty, M. (2007). Light truck vehicles contribution to rear - end collisions. *Accident Analysis and Prevention*, 39(5), 1026–1036.
- Harmati, I.A., Rovid, A., Szeidl, L., and Varlaki, P. (2008). Energy distribution modeling of car body deformation using LPV representations and fuzzy reasoning. *WSEAS Transactions on Systems*, 7(1), 1228–1237.

- Huang, M. (2002). *Vehicle Crash Mechanics*. Boca Raton, CRC Press.
- Jonsén, P., Isaksson, E., Sundin, K.G., and Oldenburg, M. (2009). Identification of lumped parameter automotive crash models for bumper system development. *International Journal of Crashworthiness*, 14(6), 533–541.
- Karimi, H.R. and Robbersmyr, K.G. (2011). Signal analysis and performance evaluation of a vehicle crash test with a fixed safety barrier based on Haar wavelets. *International Journal of Wavelets, Multiresolution and Image Processing*, 9(1), 131–149.
- Kim, H.S., Kang, S.Y., Lee, I.H., Park, S.H., and Han, D.C. (1996). Vehicle frontal crashworthiness analysis by simplified structure modeling using nonlinear spring and beam elements. *International Journal of Crashworthiness*, 2, 107–118.
- Moumni, Z. and Axisa, F. (2004). Simplified modelling of vehicle frontal crashworthiness using a modal approach. *International Journal of Crashworthiness*, 9, 285–297.
- Omar, T., Eskandarian, A., and Bedewi, N. (1998). Vehicle crash modelling using recurrent neural networks. *Mathematical and Computer Modelling*, 28(9), 31–42.
- Pawlus, W., Nielsen, J.E., Karimi, H.R., and Robbersmyr, K.G. (2010a). Comparative analysis of vehicle to pole collision models established using analytical methods and neural networks. Accepted and to be presented at the 5th IET International System Safety Conference, Manchester, UK.
- Pawlus, W., Nielsen, J.E., Karimi, H.R., and Robbersmyr, K.G. (2010b). Further results on mathematical models of vehicle localized impact. The 3rd International Symposium on Systems and Control in Aeronautics and Astronautics, Harbin, China.
- Pawlus, W., Nielsen, J.E., Karimi, H.R., and Robbersmyr, K.G. (2010c). Mathematical modeling and analysis of a vehicle crash. The 4th European Computing Conference, Bucharest, Romania.
- Robbersmyr, K.G. (2004). Calibration test of a standard Ford Fiesta 1.1i, model year 1987, according to NS - EN 12767. Technical Report 43/2004, Agder Research, Grimstad.
- Soica, A. and Lache, S. (2007). Theoretical and experimental approaches to motor vehicle: Pedestrian collision. The 3rd WSEAS International Conference on Applied and Theoretical Mechanics, Spain.
- Soto, C.A. (2004). Structural topology optimization for crashworthiness. *International Journal of Crashworthiness*, 9, 277–284.
- Tenga, T.L., Changb, F.A., Liuc, Y.S., and Peng, C.P. (2008). Analysis of dynamic response of vehicle occupant in frontal crash using multibody dynamics method. *Mathematical and Computer Modelling*, 48, 1724–1736.
- van der Laan, E., Veldpaus, F., de Jager, B., and Steinbuch, M. (2008). LPV modeling of vehicle occupants. AVEC 08 9th International Symposium on Advanced Vehicle Control, Kobe, Japan.
- Varat, M.S. and Husher, S.E. (2000). Crash pulse modeling for vehicle safety research. 18th ESV.
- Várkonyi-Kóczy, A.R., Rövid, A., and Várlaki, P. (2004). Intelligent methods for car deformation modeling and crash speed estimation. The 1st Romanian - Hungarian Joint Symposium on Applied Computational Intelligence, Timisoara, Romania.